In vivo expression of G-protein beta1gamma2 dimer in adult mouse skeletal muscle alters L-type calcium current and excitation-contraction coupling.

Norbert Weiss, Claude Legrand, Sandrine Pouvreau, Hicham Bichraoui, Bruno Allard, Gerald W. Zamponi, Michel de Waard, Vincent Jacquemond

In vivo expression of G-protein beta1gamma2 dimer in adult mouse skeletal muscle alters L-type calcium current and excitation-contraction coupling

Norbert Weiss [1] [*] , Claude Legrand [1] , Sandrine Pouvreau [1] , Hicham Bichraoui [1] , Bruno Allard [1] , Gerald W. Zamponi [2] , Michel De Waard [3] , Vincent Jacquemond [1]

[1] PICM, Physiologie intégrative, cellulaire et moléculaire CNRS : UMR5123 , Université Claude Bernard - Lyon I , Bât. R. Dubois 43, Bvd du 11 Novembre 1918 69622 VILLEURBANNE CEDEX,FR

[2] Department of Physiology and Biophysics University of Calgary , Calgary Alberta,CA

[3] GIN, Grenoble Institut des Neurosciences INSERM : U836 , CEA , Université Joseph Fourier - Grenoble I , CHU Grenoble , UJF - Site Santé La Tronche BP 170 38042 Grenoble Cedex 9,FR

* Correspondence should be adressed to: Norbert Weiss <norbert.weiss@yahoo.fr >

Abstract

A number of G-protein coupled receptors are expressed in skeletal muscle but their roles in muscle physiology and downstream effector systems remain poorly investigated. Here we explored the functional importance of the G-protein $\beta\gamma$ (G$\beta\gamma$) signaling pathway on voltage-controlled Ca^{2+} homeostasis in single isolated adult skeletal muscle fibres. A GFP-tagged $G\beta_1\gamma_2$ dimer was expressed in vivo in mice muscle fibres. The GFP fluorescence pattern was consistent with a $G\beta_1\gamma_2$ dimer localization in the transverse-tubule membrane. Membrane current and indo-1 fluorescence measurements performed under voltage-clamp conditions reveal a drastic reduction of both L-type Ca^{2+} current density and of peak amplitude of the voltage-activated Ca^{2+} transient in $G\beta_1\gamma_2$ -expressing fibres. These effects were not observed upon expression of $G\beta_2\gamma_2$, $G\beta_3\gamma_2$ or $G\beta_4\gamma_2$. Our data indicate that the G-protein $\beta_1\gamma_2$ dimer plays an important regulatory role in excitation-contraction coupling.

Introduction

G-protein coupled receptors (GPCRs) represent a large family of cell plasma membrane receptors that are involved in the transduction of extracellular signals into cellular responses (for review see (Milligan & Kostenis, 2006)). Activation of GPCRs following extracellular agonist stimulation results in the activation of two intracellular signaling molecules, Gα-GTP and the free G$\beta\gamma$ dimer. Whereas Gα -dependent signaling pathways involve the activation of soluble messenger cascades such as adenylyl cyclases, cyclic GMP phosphodiesterases or phospholipases Cβ, G$\beta\gamma$-mediated regulation generally occurs through direct binding of the dimer to target effectors. One such class of targeted receptors is represented by voltage-gated calcium channels (for review see (McCudden et al. , 2005)).

In skeletal muscle, no less than 43 GPCRs were found to be expressed at the protein or mRNA level. Signaling activity of this GPCRs is suspected to play a role in the regulation of several aspects of muscle physiology, including plasticity, differentiation, pain, but also more specifically in the control of glucose uptake and of ion transport and membrane excitability (for review see (Jean-Baptiste et al. , 2005)). Early sets of data also suggested that G-proteins may be involved in the regulation of excitation-contraction (E-C) coupling process. In skeletal muscle E-C coupling relies on a tight control of sarcoplasmic reticulum (SR) Ca^{2+} release through the type 1 ryanodine receptor (RyR1) by the voltage-sensing dihydropyridine receptor (DHPR)/Ca_v 1.1 Ca^{2+} channel. Activation of the Ca_v 1.1 subunit in response to transverse (t-) tubule membrane depolarization directly activates RyR1, allowing rapid mobilization of the SR Ca^{2+} store and the rise in myoplasmic Ca^{2+} concentration that triggers contraction (for review see (Dulhunty, 2006)). A possible functional role of GPCR signaling in the regulation of E-C coupling was suggested by experiments in skinned skeletal muscle fibres in which it was shown that constitutive activation of G-proteins by GTPγS either enhanced calcium- or caffeine-induced calcium release (Villaz et al. , 1989) or directly elicited fibre contraction (Di Virgilio et al. , 1986 ; Somasundaram et al. , 1991). Furthermore, GTPγS was also reported to increase DHPR-L-type Ca^{2+} current and intramembrane charge movement measured under vaseline-gap voltage-clamp conditions in rat and frog cut skeletal muscle fibres (Garcia et al. , 1990). However, the issue became controversial as Lamb and Stephenson (Lamb & Stephenson, 1991) found no effect of GTPγS on both depolarization-induced Ca^{2+} release in skinned rat fibres and on intramembrane charge movement in rat cut fibres. Differences in the experimental conditions between these studies are most likely responsible for these discrepancies. Nevertheless, the use of GTPγS under such conditions remains a rather limited approach. First, in both skinned and cut fibre

preparations, critical diffusible factors may potentially be washed out of the myoplasmic compartment, possibly precluding proper G-protein signaling. Second, GTPγS will not discriminately activate all G-protein signaling in the cell, thus come placating interpretations at the mechanistic level. Finally, along the same lines, GTPγS is expected to stimulate both Gα- and Gβγ-signaling pathways thus further hampering the interpretation of experimental results. Interestingly, recent data on cultured myotubes showed that direct extracellular application of the calcitonin gene-related peptide (CGRP) enhanced voltage-gated Ca^{2+} release, L-type calcium currents and charge movements (Avila et al. , 2007). This then supports a functional role of GPCRs in regulating Ca^{2+} influx through Ca_v 1.1 and thus potentially E-C coupling.

The aim of the present study was to specifically test the role of the G-protein βγ complex in the control of Ca^{2+} homeostasis in skeletal muscle fibres from mouse. We investigated the effects of the functional G-protein $β_1$ $γ_2$ dimer on the Ca^{2+} channel properties of the DHPR, as well as on those of the voltage-activated Ca^{2+} transients in fully differentiated adult skeletal muscle fibres. Our results suggest that the G-protein $β_1$ $γ_2$ dimer is targeted to the T-tubule membrane system where it modulates Ca^{2+} homeostasis by inhibiting the ion channel function of the DHPR and the voltage-activated SR Ca^{2+} release process. Our findings thus provide novel evidence for an efficient G-protein-dependent regulatory mechanism of E-C coupling in adult skeletal muscle.

Materials and Methods

Ethical approval

All experiments and procedures were performed in accordance with the guidelines of the local animal ethics committee of University Lyon 1, of the French Ministry of Agriculture (87/848) and of the European Community (86/609/EEC).

Plasmid cDNAs

Plamid cDNAs encoding for GFP-tagged $Gβ_{1-4}$ and $Gγ_2$ were created and tagged as described by us previously (Arnot et al. , 2000 ; Feng et al. , 2001).

In vivo cDNA electroporation

Experiments were performed using 4- to 8-week-old male OF1 mice (Charles River Laboratories, L'Arbresle, France). In vivo cDNA electroporation was performed as previously described (Weiss et al. , 2008). Mice were anesthetized by i.p. injection of 10 μL/g of a mixture of 5% ketamine (Merial, Lyon, France) and 2% xylazine (Bayer, Kiel, Germany). A 50 μL volume of 10 μg/μL of the plasmid mix cDNAs encoding for the GFP-tagged Gβ construct (GFP-$Gβ_1$, GFP-$Gβ_2$, GFP-$Gβ_3$ or GFP-$Gβ_4$) along with the G-protein $γ_2$ subunit was injected within the ventral side of the posterior paws through a 29-gauge needle (Terumo, Leuven, Belgium). The paw was then placed between two flat platinum electrodes, and 8 pulses of 200 V/cm amplitude of 20 ms duration were applied at 1 Hz (ECM 830 Electro Square Porator, BTX).

Isolation and preparation of FDB muscle fibres

Experiments were performed on single skeletal fibres isolated from the flexor digitorum brevis (FDB) muscles 5 days after electroporation. Procedures for enzymatic isolation of single fibres, partial insulation of the fibres with silicone grease and intracellular dye loading were as previously described (Jacquemond, 1997 ; Collet et al. , 1999 ; Collet & Jacquemond, 2002 ; Collet et al. , 2004). In brief, mice were killed by cervical dislocation after isofluoran (Sigma Aldrich, Saint Quentin Fallavier, France) inhalation, before removal of the muscles. Muscles were treated with 2 mg/mL collagenase type-1 (Sigma Aldrich) in Tyrode solution (see Solutions) for 60 min at 37°C. Single fibres were then isolated by triturating the muscles within the experimental chamber. Fibres expressing the $Gβ_x$ $γ_2$ dimers were identified from the GFP fluorescence. The major part of a single fibre was then electrically insulated with silicone grease (Rhodia Siliconi Italia, Treviolo, Italy) so that whole-cell voltage-clamp could be achieved on a short portion of the fibre extremity. As previously reported upon expression of exogenous ryanodine receptors (Legrand et al. , 2008) one hallmark of the expression pattern of the Gβγ dimers was that it was not homogenous throughout the muscle fibres but most usually restricted within one given portion of the fibres, around a nucleus. Transfected fibres thus had to be handled with silicone so that the fibre region exhibiting GFP fluorescence was left out of the silicone. However, not all GFP-positive fibres were amenable to this procedure, especially when the region of expression was within the central portion of the fibre. More importantly, in most cases the total portion of fibre left out of silicone was not 100% GFP-positive so that any effect due to the expressed Gβγ dimer was likely to be underestimated in the silicone-free portion of the fibre for measurements of whole-cell membrane currents and indo-1 fluorescence.

Confocal imaging

Confocal images of the GFP fluorescence and di-8-ANEPPS (10 μM, Invitrogen) labeling on freshly isolated fibres were obtained on a Zeiss LSM 5 laser scanning confocal microscope. The microscope was equipped with a ×63 oil immersion objective (numerical aperture 1.4). All experiments were performed at room temperature (20–22°C).

Electrophysiology

An RK-400 patch-clamp amplifier (Bio-logic, Claix, France) was used in whole-cell configuration. Command voltage pulse generation and data acquisition were done using WinWCP software (freely provided by Dr. Dempster, University of Strathclyde, Glasgow, Scotland) driving an A/D, D/A converter (National Instruments, Austin, TX, USA). Analog compensation was systematically used to decrease the effective series resistance. Voltage-clamp was performed with a microelectrode filled with an internal-like solution (see Solutions) of 1–3 MΩ resistance. The tip of the microelectrode was inserted through the silicone within the insulated part of the fibre. Membrane depolarization were applied every 30 sec from a holding command potential of −80 mV. A 30 sec pulse interval allows the total recovery of DHPRs from the inactivated state (Collet et al. , 2003).

Measurement of calcium currents

Voltage-activated Ca^{2+} currents were recorded in response to 1-sec-long depolarizing steps to various potentials. The linear leak component of the current was removed by subtracting the adequately scaled value of the steady current measured during a 20 mV hyperpolarizing step applied before each test pulse. The voltage-dependence of the peak Ca^{2+} current density was fitted with the following modified Boltzman equation: $I(V) = G_{max} (V − V_{rev})/(1 + exp[(V_{1/2} − V)/k]$, with I (V) being the peak current density at the command potential V , G_{max} the maximum conductance, V_{rev} the reverse potential, $V_{1/2}$ the half-activation potential and k the steepness factor. The voltage-dependence of the whole-cell Ca^{2+} conductance was calculated using the following modified Boltzman equation: $G(V) = G_{max}/(1 + exp(−(V − V_{1/2})/k))$, with G(V) being the Ca^{2+} conductance at the command potential V .

Ca^{2+} transients measurements using indo-1

Prior to voltage-clamp, the indo-1 dye, diluted at a concentration of 0.2 mM in an intracellular-like solution (see Solutions), was dialyzed into the fibre cytoplasm with the microelectrode solution inserted through the silicone, within the insulated part of the fibre. In order to ease intracellular dialysis, the electrode tip was crushed within the silicon-insulated portion of the fibre by pushing it back and forth a few times towards the bottom of the chamber. Intracellular equilibration of the solution was allowed for a period of 30 min before initiating measurements. Indo-1 fluorescence was measured on an inverted Nikon Diaphot epifluorescence microscope equipped with a commercial optical system, allowing the simultaneous detection of fluorescence at 405 nm (F_{405}) and 485 nm (F_{485}) by two photomultipliers (IonOptix, Milton, MA, USA) upon 360-nm excitation. Background fluorescence at both emission wavelengths was measured next to each fibre tested and was then subtracted from all measurements.

Calibration of the indo-1 response and $[Ca^{2+}]_{intra}$ calculation

The standard ratio method was used with the parameters: $R = F_{405}/F_{485}$, with R_{min} , R_{max} , K_D and β having their usual definitions. Results were either expressed in terms of indo-1 % saturation or in actual free Ca^{2+} concentration (for details of calculation see (Jacquemond, 1997 ; Csernoch et al. , 1998)). In vivo values for R_{min} , R_{max} and β were measured using procedures previously described (Collet et al. , 1999 ; Collet & Jacquemond, 2002). Corresponding mean values were 0.239 ± 0.004 (n=9), 1.783 ± 0.028 (n=9) and 2.128 ± 0.014 (n=13), respectively. No correction was made for indo-1-Ca^{2+} binding and dissociation kinetics. As a consequence, the calculated Ca^{2+} transients do not scrupulously reflect the true time course of change in free calcium. This, however, will not influence any of the conclusions from the present study (for details, see (Jacquemond, 1997)).

Solutions

The intracellular-like solution contained (in mM): 120 potassium glutamate, 5 Na_2 -ATP, 5 Na_2 -phosphocreatine, 5.5 $MgCl_2$, 5 D-glucose and 5 HEPES adjusted to pH 7.2 with KOH. The standard extracellular solution contained (in mM): 140 TEA-methanesulphonate, 2.5 $CaCl_2$, 2 $MgCl_2$, 0.002 TTX and 10 HEPES adjusted to pH 7.2. For measurement of the slow Ca^{2+} current, the extracellular solution contained also 1 mM 4-aminopyridine and 5 $CaCl_2$, and fibres were incubated with 0.1 mM EGTA-AM during 30 min before starting the experiment. The Tyrode solution contained (in mM): 140 NaCl, 5 KCl, 2.5 $CaCl_2$, 2 $MgCl_2$ and 10 HEPES adjusted to pH 7.2 with NaOH.

Statistics

Least-squares fits were performed using a Marquardt-Levenberg algorithm routine included in Microcal Origin (OriginLab, Northampton, MA, USA). Data values are presented as mean ± S.E.M. for n fibres tested, where n is specified in Results . Statistical significance was determined using Student's t test: *, p<0.05; **, p<0.01; ***, p<0.001; NS, statistically not different.

Results

In vivo expression of the GFP-tagged G-protein $β_1 γ_2$ dimer in adult mouse skeletal muscle fibres

Under the conditions of fibre electroporation used in this study (for details see Materials and Methods), a restricted number of fibers (typically 10 to 20) were found to express the G-protein β_1 -GFPγ_2 dimer out of the total population of fibres isolated from one given transfected FDB muscle. Fig. 1 shows an example of the typical expression pattern of the GFP-G$\beta_1 \gamma_2$ dimer observed under confocal microscopy. The GFP-G$\beta_1 \gamma_2$ dimer yielded a repetitive double-row pattern perpendicular to the longitudinal axis of the fibre, consistent with the T-tubule membrane system. This was confirmed by the strong co-localization of the GFP fluorescence with the di-8-ANNEPS membrane straining (Fig. 1C–D). These observations indicate the proper localization of the G-protein $\beta_1 \gamma_2$ dimer with regard to the excitation-contraction coupling machinery (Tanaka et al. , 2000).

In vivo expression of the GFP-tagged G-protein $\beta_1 \gamma_2$ dimer reduces L-type calcium current density

To investigate the effect of G-protein $\beta_1 \gamma_2$ dimer on the ionic properties of the Ca_v 1.1 calcium channel, L-type calcium currents were recorded in G-protein $\beta_1 \gamma_2$ dimer-expressing fibres. Representative Ca^{2+} current traces recorded in response to 1 sec long depolarizing steps to values ranging between −50 mV and +80 mV, from a holding potential of −80 mV, are shown in Fig. 2A in a control fibre (left panel) and in a G$\beta_1 \gamma_2$ dimer-expressing fibre (right panel). Control fibres were GFP-negative fibres issued from the same muscles. Fig. 2B shows the mean peak Ca^{2+} current density as a function of membrane voltage for control (filled circle) and G$\beta_1 \gamma_2$ dimer-expressing fibres (open circle). The L-type Ca^{2+} current density was significantly reduced in fibres expressing the G$\beta_1 \gamma_2$ dimer. For instance, in response to a depolarizing pulse to +10 mV, the mean peak Ca^{2+} current density was decreased by 40% (p =0.0004) in G$\beta_1 \gamma_2$ -expressing fibres (−5.9 ± 1.1 A/F, n =6) compared to control fibres (−9.8 ± 0.4 A/F, n =25). The voltage-dependence of the L-type Ca^{2+} current activation was also determined in control and in G$\beta_1 \gamma_2$ -expressing fibres (Fig. 2B , inset). The mean half-activation potential remained unaltered (p =0.26) in G$\beta_1 \gamma_2$ -expressing fibres (−2.3 ± 2.8 mV, n =6) compared to control fibres (−5.0 ± 0.9 mV, n =25). The mean corresponding conductance versus membrane potential relationships are presented in Fig. 2C for control fibres (filled circles) and G$\beta_1 \gamma_2$ -expressing fibres (open circles). The maximal conductance (Fig. 2C , inset) was reduced by 35% (p =0.001) in G$\beta_1 \gamma_2$ -expressing fibres (103 ± 11 S/F, n =6) as compared to control fibres (159 ± 7 S/F, n =25). Electroporation itself had no effect on the L-type Ca^{2+} current density (data not shown). We also tested the capability of other G-protein β subunit isoforms to modulate L-type Ca^{2+} currents. Representative current traces from fibres expressing G$\beta_2 \gamma_2$ (top panel), G$\beta_3 \gamma_2$ (middle panel) and G$\beta_4 \gamma_2$ (bottom panel) are shown in Fig. 3 . Corresponding mean values for peak Ca^{2+} current densities and conductances as a function of membrane potential are shown in Fig. 3B and 3C , respectively. No significant alteration of these parameters was observed. For instance, neither the mean half-activation potential of the L-type Ca^{2+} current, nor the maximal conductance was changed. Taken together, these data demonstrate that the L-type Ca^{2+} current is specifically altered by the G-protein $\beta_1 \gamma_2$ dimer in adult skeletal muscle fibres.

Expression of the G-protein $\beta_1 \gamma_2$ dimer slows down activation and inactivation kinetics of the L-type calcium current

To further investigate the functional impact of G-protein $\beta_1 \gamma_2$ expression on the Ca_v 1.1 channel, the kinetics of L-type Ca^{2+} currents were analyzed in control and G$\beta_1 \gamma_2$ -expressing fibres. Fig. 4A shows normalized Ca^{2+} current traces obtained in response to 1 sec long depolarizing steps to +10 mV (left panel) and +30 mV (right panel) from a holding potential of −80 mV, in a control fibre (top panel) and in a G$\beta_1 \gamma_2$ -expressing fibre (bottom panel). We found that the Ca^{2+} current activation was slowed in fibres expressing the G$\beta_1 \gamma_2$ dimer as evidenced by larger time-to-peak values, which was particularly pronounced at the lowest voltage tested (Fig. 4B). For instance, in response to a depolarizing step to +10 mV, the time-to-peak of the Ca^{2+} current recorded from G$\beta_1 \gamma_2$ -expressing fibres was, on average, 1.5-fold greater than in control fibres (205 ± 30 ms, n =6, versus 137 ± 6 ms, n =25, respectively, p =0.001). This slowing remained significant for depolarizing steps levels up to +40 mV. The time course of Ca^{2+} current inactivation was determined by fitting the inactivating phase of the current by a single exponential function (Fig. 4A , bold lines). Mean corresponding values for the time constant (τ) are presented in Fig. 4C for control (filled circles) and G$\beta_1 \gamma_2$ -expressing fibres (open circles). As shown in the figure, in response to a depolarizing step to +10 mV, the time constant of Ca^{2+} current inactivation in G$\beta_1 \gamma_2$ -expressing fibres was, on average, 1.7-fold greater than in control fibres (262 ± 46 ms, n =6, versus 156 ± 12 ms, n =25, p =0.003). This slowing remained significant for depolarizing steps levels up to +30 mV.

Effect of a strong depolarizing prepulse on the regulation of the L-type calcium current by G-protein $\beta_1 \gamma_2$ dimer

It is well known that application of strong depolarizing prepulses under direct G-protein regulation of voltage-gated Ca^{2+} channels produces either a current facilitation, and/or a change in kinetics of the Ca^{2+} current (Scott & Dolphin, 1990 ; Ikeda, 1991). Representative Ca^{2+} current traces in response to a 1 sec long depolarizing step to +20 mV from a holding potential of −80 mV, before (P1) and after (P2) a strong 100 ms long depolarizing prepulse to +100 mV are shown in Fig. 5A in a control fibre (left panel) and in a G$\beta_1 \gamma_2$ -expressing fibre (right panel). The normalized peak Ca^{2+} current amplitude recorded before and after the depolarizing prepulse (P2/P1) was plotted as a function of the duration of the prepulse in control (filled circles, n =13) and G$\beta_1 \gamma_2$ -expressing fibres (open circles, n =6) (Fig. 5B). As

shown in the figure, there was either no prepulse-induced current recovery from G-protein inhibition or the effect was sufficiently small to be masked by the inactivation of the Ca^{2+} current induced by the depolarizing prepulse. The time-to-peak of the current plotted as a function of the duration of the depolarizing prepulse is shown in Fig. 5C . A clear convergence of the values recorded in $G\beta_1 \gamma_2$ -expressing fibres towards the values recorded in control fibres is observed. Interestingly, the corresponding mean values of the shift in current time-to-peak between control fibres and $G\beta_1 \gamma_2$ expressing fibres clearly indicates a recovery from the process of $G\beta_1 \gamma_2$ -induced slowing of Ca^{2+} current activation (Fig. 5D). This suggests that the effect of the G-protein $\beta_1 \gamma_2$ dimer on the L-type Ca2+ current could occur, at least partially, via the binding of the $G\beta_1 \gamma_2$ dimer to the $Ca_v 1.1$ subunit.

G-protein $\beta_1 \gamma_2$ dimer expression alters voltage-activated calcium transients

In order to further investigate the possible functional role of G-proteins in the control of excitation-contraction coupling and, from a more general point of view, in the control of intracellular Ca^{2+} homeostasis, Ca^{2+} transients were recorded in control and $G\beta_1 \gamma_2$ -expressing fibres under voltage-clamp conditions. Representative indo-1 saturation traces from a control (left panel) and from a $G\beta_1 \gamma_2$ -expressing fibre (left panel), in response to successive depolarizing pulses of 5, 10, 20, 50 and 100 ms duration to +10 mV from a holding potential of −80 mV are shown in Fig. 6A . Corresponding $[Ca^{2+}]$ traces calculated from the indo-1 signals are shown in Fig. 6B . Obviously, the amplitude of the Ca^{2+} transients was dramatically diminished in the $G\beta_1 \gamma_2$ -expressing fibre. Fig. 6C–F show mean values from that series of measurements for resting $[Ca^{2+}]$, peak $\Delta[Ca^{2+}]$, time constant (τ) of $[Ca^{2+}]$ decay and final $\Delta[Ca^{2+}]$ in control (filled circle, n =10) and $G\beta_1 \gamma_2$ -expressing fibres (open circle, n =6). Measurements were performed on individual $[Ca^{2+}]$ traces calculated from each fibre. The time constant of decay was obtained from fitting a single exponential plus constant function to the $[Ca^{2+}]$ decline. In response to a depolarizing step of 20 ms long duration, the mean peak $\Delta[Ca^{2+}]$ was 43% less (p =0.0003) in $G\beta_1 \gamma_2$ -expressing fibres (0.63 ± 0.10 µM, n =6) than in control ones (1.11 ± 0.05 µM, n =10). No significant differences in any of the other parameters (resting $[Ca^{2+}]$, time constant (τ) of $[Ca^{2+}]$ decay and final $\Delta[Ca^{2+}]$) were detected between control and $G\beta_1 \gamma_2$ -expressing fibres. Taken together, these results indicate that expression of the G-protein $\beta_1 \gamma_2$ dimer dramatically alters voltage-induced Ca^{2+} release without affecting the ability of the cells to regulate the Ca^{2+} concentration at rest.

Discussion

We demonstrate that expression of the G-protein $\beta_1 \gamma_2$ dimer in intact adult mammalian skeletal muscle fibres alters both the Ca^{2+} channel function of the DHPR and the process of voltage-activated Ca^{2+} release from the SR. These effects are specific of the $G\beta_1$ isoform as no alteration was observed when the $G\beta_2 \gamma_2$, $G\beta_3 \gamma_2$ or $G\beta_4 \gamma_2$ dimers were expressed. This subtype selectivity strongly argues against a transfection artifact and supports the ability of $Ca_v 1.1$ channels to undergo G-protein inhibition. The in vivo expression of the G-protein $\beta_1 \gamma_2$ dimer in adult mouse muscle was successful and yielded a very distinct subcellular pattern consistent with a specific localization of the dimer in the T-tubule membrane system. This observation nicely fits with previous biochemical studies showing the presence of the G-protein β subunits in T-tubule membrane preparations purified from rabbit skeletal muscle (Toutant et al. , 1988), as well as with immunostaining of endogenous G-protein β subunits, also in rabbit skeletal muscle (Toutant et al. , 1990).

Possible mechanism of G-protein $\beta_1 \gamma_2$ modulation of the L-type Ca^{2+} current

Previous studies aiming at exploring the role of G-proteins on E-C coupling in adult muscle used GTPγS on either skinned skeletal muscle fibre preparations (Di Virgilio et al. , 1986 ; Lamb & Stephenson, 1991 ; Somasundaram et al. , 1991) or vaseline-gap voltage-clamped cut fibres (Garcia et al. , 1990), which provided controversial results. As detailed earlier, the use of GTPγS under such conditions is a somewhat limiting strategy. In this context, the in vivo expression of exogenous functional G-protein $\beta_1 \gamma_2$ dimer in intact fully differentiated muscle fibres provides a more defined and specific approach. In particular, it should bypass the possible consequences of activation of multiple endogenous G-protein signaling pathways.

On average, $G\beta_1 \gamma_2$ positive fibres yielded a decrease in Ca^{2+} current amplitude corresponding to a 35% drop in peak conductance. This is a very substantial alteration, especially considering that it is likely to be heavily underestimated because of the local expression of the G$\beta_1 \gamma_2$ dimer within the whole-cell voltage-clamped portion of fibre (see Methods). The G-protein βγ dimer is known to directly regulate neuronal voltage-gated Ca^{2+} channels ($Ca_v 2.1$, $Ca_v 2.2$ and $Ca_v 2.3$) (for review see (De Waard et al. , 2005 ; Tedford & Zamponi, 2006)) through direct binding of the Gβγ dimer onto various structural elements of the $Ca_v 2.x$ subunit. Those include the loop linking transmembrane domains I and II (De Waard et al. , 1997 ; Zamponi et al. , 1997), the amino-terminal (Agler et al. , 2005) and possibly the carboxy-terminal domain (Qin et al. , 1997).

Present results showing a prepulse dependent reversal of some of the kinetic effects strongly suggest that $Ca_v 1.1$ L-type channels can also be directly regulated by G-proteins, although we do not presently have biochemical evidence to demonstrate a protein-protein

interaction. It was initially thought that Ca_v 1.x channels are not subject to direct G-protein regulation because they lack the Gβγ binding QXXER domain present in the I–II loop of Ca_v 2.x channels and absent in Ca_v 1.x channels. However, more recently, it was demonstrated that the Ca_v 1.2 channel is sensitive to G-protein inhibition through a direct binding of the Gβγ dimer onto the amino- and carboxy-terminal domains of the channel (Ivanina et al. , 2000).

The so far limited amount of evidence concerning G-protein regulation of Ca_v 1.1 L-type channels is likely related to difficulty in heterologous expression of Ca_v 1.1 channels. Here, the fully differentiated skeletal muscle fibre preparation allowed detailed investigation of the role of the G-protein βγ dimer on the Ca_v 1.1 channel activity. Although we cannot totally exclude that over-expression of $Gβ_1 γ_2$ may have activated another signal transduction pathway to modulate Ca_v 1.1 activity, several considerations argue against such mechanism. First, the effect is specific as only the G-protein $β_1$ subunit modulated channel activity. This is reminiscent of data obtained with the Ca_v 3.2 T-type channel which was shown to be solely mediated by the G-protein $β_2$ subunit, with other Gβ subunits being ineffective (Wolfe et al. , 2003 ; DePuy et al. , 2006). Second, the slowing of activation and inactivation kinetics of L-type Ca^{2+} currents in $Gβ_1 γ_2$ -expressing fibres, and its reversal by a depolarizing prepulse fits with the idea of direct G-protein regulation (Marchetti et al. , 1986 ; Scott & Dolphin, 1990 ; Ikeda, 1991 ; Zamponi, 2001). Finally, previous biochemical studies suggested that the G-protein β subunit associates with the DHPR, although the molecular determinants involved in this interaction remained unidentified (Hamilton et al. , 1991). Altogether, we favor the idea of a direct G-protein regulation of the DHPR Ca^{2+} channel activity.

Possible mechanism of G-protein $β_1 γ_2$ modulation of the excitation-contraction coupling

Functional coupling between the DHPR and RyR1 occurs through direct or indirect interactions of possibly several cytosolic determinants of Ca_v 1.1 with RyR1 (for recent review see (Bannister, 2007)). Among them the II–III loop is established to play a key role in E-C coupling (Tanabe et al. , 1990 ; Lu et al. , 1994) and alteration of the corresponding interaction alters both the L-type Ca^{2+} current density and the amplitude of the voltage-activated Ca^{2+} transient (Bannister et al. , 2009). Other structural determinants of the Ca_v 1.1 subunit postulated to be involved in the regulation of E-C coupling include the I–II loop (via the voltage-gated Ca^{2+} channel $β_{1a}$ subunit (Gregg et al. , 1996 ; Strube et al. , 1996), the carboxy-terminal domain (Slavik et al. , 1997 ; Sencer et al. , 2001) and, although likely less critical, the III–IV loop (Leong & MacLennan, 1998 ; Weiss et al. , 2004). As there is no evidence of G-protein βγ dimer interaction with RyR1, the inhibition of voltage-activated Ca^{2+} release observed in the $Gβ_1 γ_2$ -expressing fibres is probably not the consequence of a direct regulation of RyR1, but may instead be mediated by the binding of the dimer to the Ca_v 1.1 subunit. Moreover, our observation that the expression of G-protein $β_1 γ_2$ dimer alters both the L-type Ca^{2+} current and the voltage-activated Ca^{2+} release is suggestive of a common regulation mechanism. It is well known that the interaction of the II–III loop of the Ca_v 1.1 subunit with RyR1 is responsible of a bidirectional coupling: i) an orthograde coupling characterized by a voltage-induced Ca^{2+} release via RyR1, and ii) a retrograde coupling manifested by an increase of the L-type Ca^{2+} current via the DHPR (Grabner et al. , 1999). Hence, it is tempting to propose that G-protein $β_1 γ_2$ dimer may control simultaneously the L-type Ca^{2+} current and the voltage-activated Ca^{2+} release by modulating the bidirectional coupling between the DHPR and RyR1.

Potential physiological consequences of $Gβ_1 γ_2$ modulation of Ca_v 1.1

Our data raise the intriguing possibility that the $Gβ_1 γ_2$ -mediated inhibition of E-C coupling revealed here could be triggered by the activation of specific GPCRs that are coupled selectively to $Gβ_1 γ_2$. Many GPCRs are expressed or presumably expressed in skeletal muscle, with some of them being devoid of known agonists (Jean-Baptiste et al. , 2005). Hence, identification of GPCRs involved in G-protein-mediated inhibition of E-C coupling, and of their respective extracellular agonists represents an important challenge. Finally, a functional association of G-protein βγ dimer with the dystrophin glycoprotein complex (DGC) was shown to be present in skeletal muscle (Xiong et al. , 2009). One then could raise the possibility that disruption of the DGC in muscular dystrophies (for review see (Durbeej & Campbell, 2002)) may release free Gβγ dimer which in turn could alter Ca^{2+} homeostasis and excitation-contraction coupling and contribute to muscle diseases.

Overall, our data constitute the first description of Ca_v 1.1 modulation by G-protein βγ subunits. While further work will be required to ascertain its consequences for E-C coupling, the direct modulation of Ca_v 1.1 by this pathway may provide a previously unrecognized means of regulating muscle physiology.

References:

- Agler HL , Evans J , Tay LH , Anderson MJ , Colecraft HM , Yue DT . 2005 ; G protein-gated inhibitory module of N-type (ca(v)2.2) ca2+ channels . Neuron . 46 : 891 - 904

- Arnot MI , Stotz SC , Jarvis SE , Zamponi GW . 2000 ; Differential modulation of N-type 1B and P/Q-type 1A calcium channels by different G protein subunit isoforms . The Journal of physiology . 527 : (Pt 2) 203 - 212

- Avila G , Aguilar CI , Ramos-Mondragon R . 2007 ; Sustained CGRP1 receptor stimulation modulates development of EC coupling by cAMP/PKA signalling pathway in mouse skeletal myotubes . The Journal of physiology . 584 : 47 - 57

- Bannister RA . 2007 ; Bridging the myoplasmic gap: recent developments in skeletal muscle excitation-contraction coupling . J Muscle Res Cell Motil . 28 : 275 - 283

- Bannister RA , Papadopoulos S , Haarmann CS , Beam KG . 2009 ; Effects of inserting fluorescent proteins into the alpha1S II–III loop: insights into excitation-contraction coupling . The Journal of general physiology . 134 : 35 - 51

- Collet C , Allard B , Tourneur Y , Jacquemond V . 1999 ; Intracellular calcium signals measured with indo-1 in isolated skeletal muscle fibres from control and mdx mice . The Journal of physiology . 520 : (Pt 2) 417 - 429

- Collet C , Csernoch L , Jacquemond V . 2003 ; Intramembrane charge movement and L-type calcium current in skeletal muscle fibers isolated from control and mdx mice . Biophysical journal . 84 : 251 - 265

- Collet C , Jacquemond V . 2002 ; Sustained release of calcium elicited by membrane depolarization in ryanodine-injected mouse skeletal muscle fibers . Biophysical journal . 82 : 1509 - 1523

- Collet C , Pouvreau S , Csernoch L , Allard B , Jacquemond V . 2004 ; Calcium signaling in isolated skeletal muscle fibers investigated under "Silicone Voltage-Clamp" conditions . Cell biochemistry and biophysics . 40 : 225 - 236

- Csernoch L , Bernengo JC , Szentesi P , Jacquemond V . 1998 ; Measurements of intracellular Mg2+ concentration in mouse skeletal muscle fibers with the fluorescent indicator mag-indo-1 . Biophysical journal . 75 : 957 - 967

- De Waard M , Hering J , Weiss N , Feltz A . 2005 ; How do G proteins directly control neuronal Ca2+ channel function? . Trends in pharmacological sciences . 26 : 427 - 436

- De Waard M , Liu H , Walker D , Scott VE , Gurnett CA , Campbell KP . 1997 ; Direct binding of G-protein betagamma complex to voltage-dependent calcium channels . Nature . 385 : 446 - 450

- DePuy SD , Yao J , Hu C , McIntire W , Bidaud I , Lory P , Rastinejad F , Gonzalez C , Garrison JC , Barrett PQ . 2006 ; The molecular basis for T-type Ca2+ channel inhibition by G protein beta2gamma2 subunits . Proceedings of the National Academy of Sciences of the United States of America . 103 : 14590 - 14595

- Di Virgilio F , Salviati G , Pozzan T , Volpe P . 1986 ; Is a guanine nucleotide-binding protein involved in excitation-contraction coupling in skeletal muscle? . EMBO J . 5 : 259 - 262

- Dulhunty AF . 2006 ; Excitation-contraction coupling from the 1950s into the new millennium . Clin Exp Pharmacol Physiol . 33 : 763 - 772

- Durbeej M , Campbell KP . 2002 ; Muscular dystrophies involving the dystrophin-glycoprotein complex: an overview of current mouse models . Curr Opin Genet Dev . 12 : 349 - 361

- Feng ZP , Arnot MI , Doering CJ , Zamponi GW . 2001 ; Calcium channel beta subunits differentially regulate the inhibition of N-type channels by individual Gbeta isoforms . The Journal of biological chemistry . 276 : 45051 - 45058

- Garcia J , Gamboa-Aldeco R , Stefani E . 1990 ; Charge movement and calcium currents in skeletal muscle fibers are enhanced by GTP gamma S . Pflugers Arch . 417 : 114 - 116

- Grabner M , Dirksen RT , Suda N , Beam KG . 1999 ; The II–III loop of the skeletal muscle dihydropyridine receptor is responsible for the Bi-directional coupling with the ryanodine receptor . The Journal of biological chemistry . 274 : 21913 - 21919

- Gregg RG , Messing A , Strube C , Beurg M , Moss R , Behan M , Sukhareva M , Haynes S , Powell JA , Coronado R , Powers PA . 1996 ; Absence of the beta subunit (cchb1) of the skeletal muscle dihydropyridine receptor alters expression of the alpha 1 subunit and eliminates excitation-contraction coupling . Proceedings of the National Academy of Sciences of the United States of America . 93 : 13961 - 13966

- Hamilton SL , Codina J , Hawkes MJ , Yatani A , Sawada T , Strickland FM , Froehner SC , Spiegel AM , Toro L , Stefani E . 1991 ; Evidence for direct interaction of Gs alpha with the Ca2+ channel of skeletal muscle . The Journal of biological chemistry . 266 : 19528 - 19535

- Ikeda SR . 1991 ; Double-pulse calcium channel current facilitation in adult rat sympathetic neurones . The Journal of physiology . 439 : 181 - 214

- Ivanina T , Blumenstein Y , Shistik E , Barzilai R , Dascal N . 2000 ; Modulation of L-type Ca2+ channels by gbeta gamma and calmodulin via interactions with N and C termini of alpha 1C . The Journal of biological chemistry . 275 : 39846 - 39854

- Jacquemond V . 1997 ; Indo-1 fluorescence signals elicited by membrane depolarization in enzymatically isolated mouse skeletal muscle fibers . Biophysical journal . 73 : 920 - 928

- Jean-Baptiste G , Yang Z , Khoury C , Gaudio S , Greenwood MT . 2005 ; Peptide and non-peptide G-protein coupled receptors (GPCRs) in skeletal muscle . Peptides . 26 : 1528 - 1536

- Lamb GD , Stephenson DG . 1991 ; Excitation-contraction coupling in skeletal muscle fibres of rat and toad in the presence of GTP gamma S . The Journal of physiology . 444 : 65 - 84

- Legrand C , Giacomello E , Berthier C , Allard B , Sorrentino V , Jacquemond V . 2008 ; Spontaneous and voltage-activated Ca2+ release in adult mouse skeletal muscle fibres expressing the type 3 ryanodine receptor . The Journal of physiology . 586 : 441 - 457

- Leong P , MacLennan DH . 1998 ; The cytoplasmic loops between domains II and III and domains III and IV in the skeletal muscle dihydropyridine receptor bind to a contiguous site in the skeletal muscle ryanodine receptor . The Journal of biological chemistry . 273 : 29958 - 29964

- Lu X , Xu L , Meissner G . 1994 ; Activation of the skeletal muscle calcium release channel by a cytoplasmic loop of the dihydropyridine receptor . The Journal of biological chemistry . 269 : 6511 - 6516

- Marchetti C , Carbone E , Lux HD . 1986 ; Effects of dopamine and noradrenaline on Ca channels of cultured sensory and sympathetic neurons of chick . Pflugers Arch . 406 : 104 - 111

- McCudden CR , Hains MD , Kimple RJ , Siderovski DP , Willard FS . 2005 ; G-protein signaling: back to the future . Cell Mol Life Sci . 62 : 551 - 577

- Milligan G , Kostenis E . 2006 ; Heterotrimeric G-proteins: a short history . Br J Pharmacol . 147 : (Suppl 1) S46 - 55

- Qin N , Platano D , Olcese R , Stefani E , Birnbaumer L . 1997 ; Direct interaction of gbetagamma with a C-terminal gbetagamma-binding domain of the Ca2+ channel alpha1 subunit is responsible for channel inhibition by G protein-coupled receptors . Proceedings of the National Academy of Sciences of the United States of America . 94 : 8866 - 8871

- Scott RH , Dolphin AC . 1990 ; Voltage-dependent modulation of rat sensory neurone calcium channel currents by G protein activation: effect of a dihydropyridine antagonist . Br J Pharmacol . 99 : 629 - 630

- Sencer S , Papineni RV , Halling DB , Pate P , Krol J , Zhang JZ , Hamilton SL . 2001 ; Coupling of RYR1 and L-type calcium channels via calmodulin binding domains . The Journal of biological chemistry . 276 : 38237 - 38241

- Slavik KJ , Wang JP , Aghdasi B , Zhang JZ , Mandel F , Malouf N , Hamilton SL . 1997 ; A carboxy-terminal peptide of the alpha 1-subunit of the dihydropyridine receptor inhibits Ca(2+)-release channels . Am J Physiol . 272 : C1475 - 1481

- Somasundaram B , Tregear RT , Trentham DR . 1991 ; GTP gamma S causes contraction of skinned frog skeletal muscle via the DHP-sensitive Ca2+ channels of sealed T-tubules . Pflugers Arch . 418 : 137 - 143

- Strube C , Beurg M , Powers PA , Gregg RG , Coronado R . 1996 ; Reduced Ca2+ current, charge movement, and absence of Ca2+ transients in skeletal muscle deficient in dihydropyridine receptor beta 1 subunit . Biophysical journal . 71 : 2531 - 2543

- Tanabe T , Beam KG , Adams BA , Niidome T , Numa S . 1990 ; Regions of the skeletal muscle dihydropyridine receptor critical for excitation-contraction coupling . Nature . 346 : 567 - 569

- Tanaka H , Furuya T , Kameda N , Kobayashi T , Mizusawa H . 2000 ; Triad proteins and intracellular Ca2+ transients during development of human skeletal muscle cells in aneural and innervated cultures . J Muscle Res Cell Motil . 21 : 507 - 526

- Tedford HW , Zamponi GW . 2006 ; Direct G protein modulation of Cav2 calcium channels . Pharmacol Rev . 58 : 837 - 862

- Toutant M , Barhanin J , Bockaert J , Rouot B . 1988 ; G-proteins in skeletal muscle. Evidence for a 40 kDa pertussis-toxin substrate in purified transverse tubules . The Biochemical journal . 254 : 405 - 409
- Toutant M , Gabrion J , Vandaele S , Peraldi-Roux S , Barhanin J , Bockaert J , Rouot B . 1990 ; Cellular distribution and biochemical characterization of G proteins in skeletal muscle: comparative location with voltage-dependent calcium channels . EMBO J . 9 : 363 - 369
- Villaz M , Robert M , Carrier L , Beeler T , Rouot B , Toutant M , Dupont Y . 1989 ; G-protein dependent potentiation of calcium release from sarcoplasmic reticulum of skeletal muscle . Cell Signal . 1 : 493 - 506
- Weiss N , Couchoux H , Legrand C , Berthier C , Allard B , Jacquemond V . 2008 ; Expression of the muscular dystrophy-associated caveolin-3(P104L) mutant in adult mouse skeletal muscle specifically alters the Ca(2+) channel function of the dihydropyridine receptor . Pflugers Arch . 457 : 361 - 375
- Weiss RG , O'Connell KM , Flucher BE , Allen PD , Grabner M , Dirksen RT . 2004 ; Functional analysis of the R1086H malignant hyperthermia mutation in the DHPR reveals an unexpected influence of the III–IV loop on skeletal muscle EC coupling . Am J Physiol Cell Physiol . 287 : C1094 - 1102
- Wolfe JT , Wang H , Howard J , Garrison JC , Barrett PQ . 2003 ; T-type calcium channel regulation by specific G-protein betagamma subunits . Nature . 424 : 209 - 213
- Xiong Y , Zhou Y , Jarrett HW . 2009 ; Dystrophin glycoprotein complex-associated Gbetagamma subunits activate phosphatidylinositol-3-kinase/Akt signaling in skeletal muscle in a laminin-dependent manner . J Cell Physiol . 219 : 402 - 414
- Zamponi GW . 2001 ; Determinants of G protein inhibition of presynaptic calcium channels . Cell biochemistry and biophysics . 34 : 79 - 94
- Zamponi GW , Bourinet E , Nelson D , Nargeot J , Snutch TP . 1997 ; Crosstalk between G proteins and protein kinase C mediated by the calcium channel alpha1 subunit . Nature . 385 : 442 - 446

Fig. 1

Expression of the GFP-tagged $G\beta_1 \gamma_2$ dimer in adult muscle fibres. **(A)** Confocal images of the GFP fluorescence from a fibre freshly isolated from a muscle transfected with the cDNAs coding for the GFP-$G\beta_1$ fusion protein along with the $G\gamma_2$ subunit. **(B)** di-8-ANNEPS staining. **(C)** Overlay of the two images. **(D)** Normalized mean fluorescence GFP and di-8-ANNEPS profile along the x axis of the box region superimposed to the image in **(C)** . GFP-$G\beta_1$ fusion protein yields subcellular localization consistent with the T-tubule membrane. TS , T-tubule spacing; SL , sarcomere length.
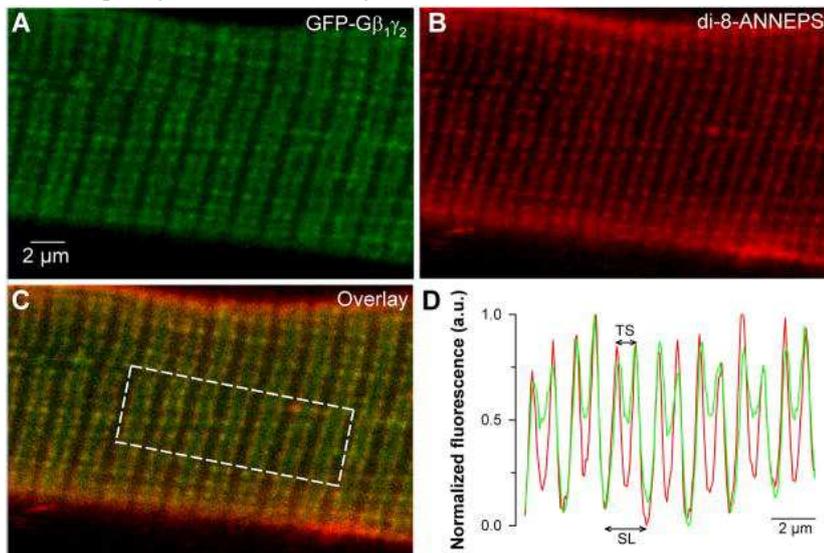
Fig. 2

Expression of G-protein $\beta_1\gamma_2$ dimers reduces L-type calcium current density in skeletal muscle fibres. **(A)** Representative sets of Ca^{2+} current traces recorded from a control (left panel) and from a $G\beta_1\gamma_2$ dimer-expressing fibre (right panel) in response to 1 sec long depolarizing steps to values ranging between −50 mV and +80 mV from a holding potential of −80 mV. **(B)** Corresponding mean voltage-dependence of the peak Ca^{2+} current density. Inset presents the mean half-maximal activation potential for control and $G\beta_1\gamma_2$ -expressing fibres. **(C)** Corresponding mean values for the voltage-dependence of Ca^{2+} conductance in the two populations. Inset presents the mean maximal conductance for control and $G\beta_1\gamma_2$ -expressing fibres. The maximal conductance was reduced by 35% (p =0.001) in the $G\beta_1\gamma_2$ -expressing fibres.
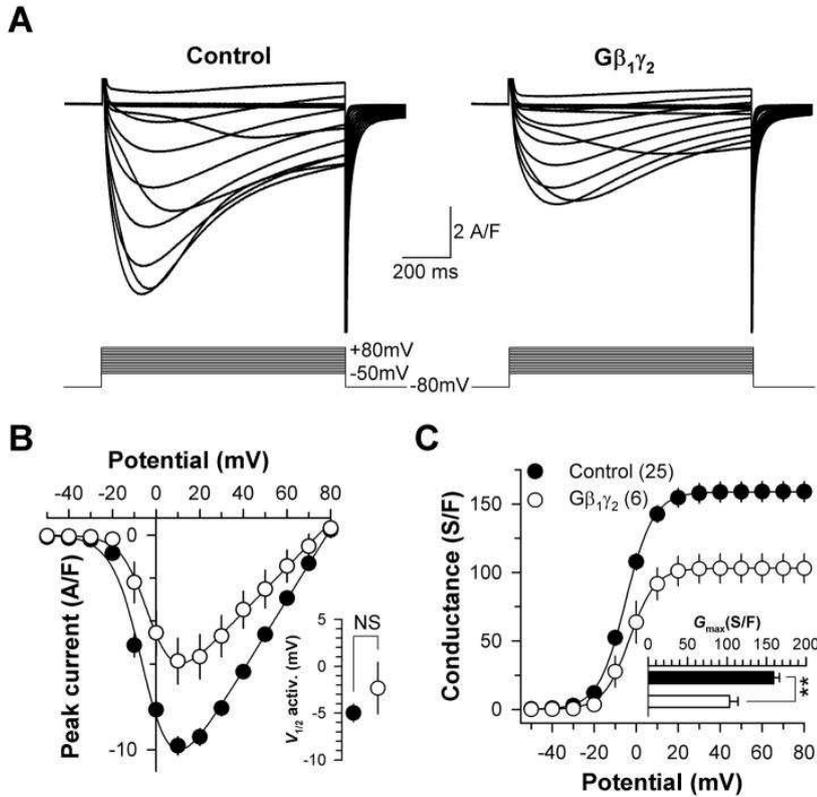
Fig. 3

Expression of G-protein $\beta_2 \gamma_2$, $\beta_3 \gamma_2$ or $\beta_4 \gamma_2$ dimers does not alter L-type calcium currents in skeletal muscle fibres. **(A)** Representative sets of Ca^{2+} current traces recorded from a $G\beta_2 \gamma_2$ (top panel), $G\beta_3 \gamma_2$ (middle panel) and $G\beta_4 \gamma_2$ (bottom panel) -expressing fibres in response to 1 sec long depolarizing steps to values ranging between −40 mV and +80 mV from a holding potential of −80 mV. **(B)** Corresponding mean voltage-dependence of the peak Ca^{2+} current density. Inset presents the mean half-maximal activation potential for $G\beta_2 \gamma_2$, $G\beta_3 \gamma_2$ and $G\beta_4 \gamma_2$ -expressing fibres. **(C)** Corresponding means values for the voltage-dependence of Ca^{2+} conductance in the three populations. Inset presents the mean maximal conductance for $G\beta_2 \gamma_2$, $G\beta_3 \gamma_2$ and $G\beta_4 \gamma_2$ -expressing fibres. The dotted line corresponds to the values from the control fibres.
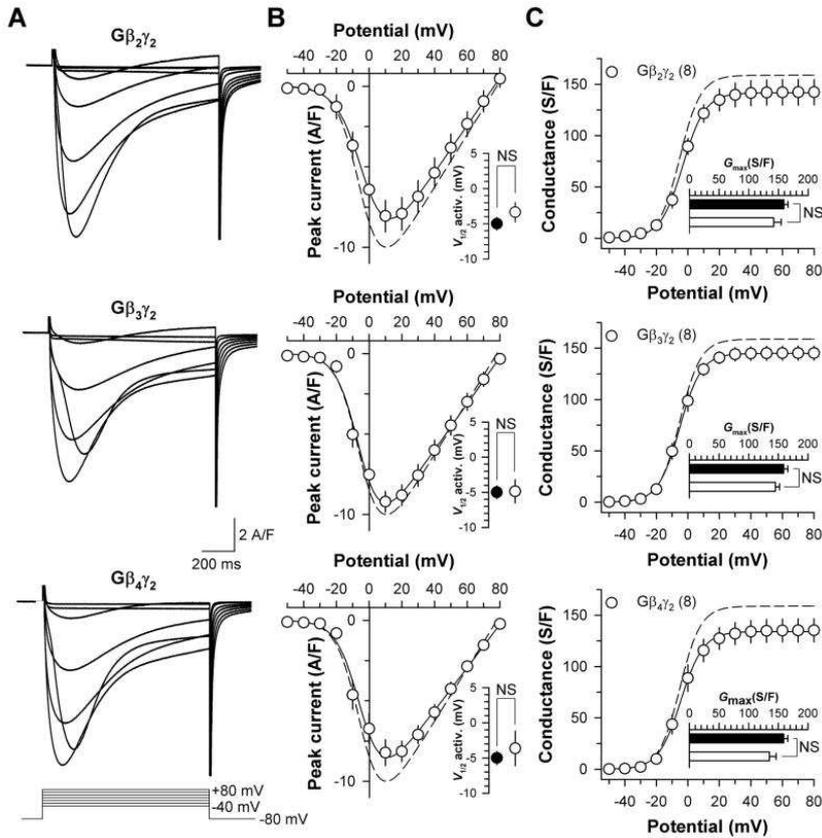
Fig. 4

Expression of G-protein $\beta_1 \gamma_2$ dimers slows down L-type calcium current activation and inactivation kinetics. **(A)** Normalized Ca^{2+} current traces recorded from a control (top panel) and from a $G\beta_1 \gamma_2$ dimer-expressing fibre (bottom panel) in response to 1 sec long depolarizing steps to **+10** mV (left panel) and **+30** mV (right panel) from a holding potential of −80 mV. The continuous superimposed bold lines correspond to the results from fitting a single exponential function to the inactivating phase of the current. **(B)** Mean values for the time-to-peak of the Ca^{2+} current for control and $G\beta_1 \gamma_2$ dimer-expressing fibres. The y axis presents a break point for display purposes. Values were significantly increased in the $G\beta_1 \gamma_2$ dimer-expressing fibres for potential values from 0 mV to +40 mV. **(C)** Mean values for the time constant τ of Ca^{2+} current inactivation. Values were significantly increased in the $G\beta_1 \gamma_2$ dimer-expressing fibres at potentials ranging from 0 mV to +30 mV.
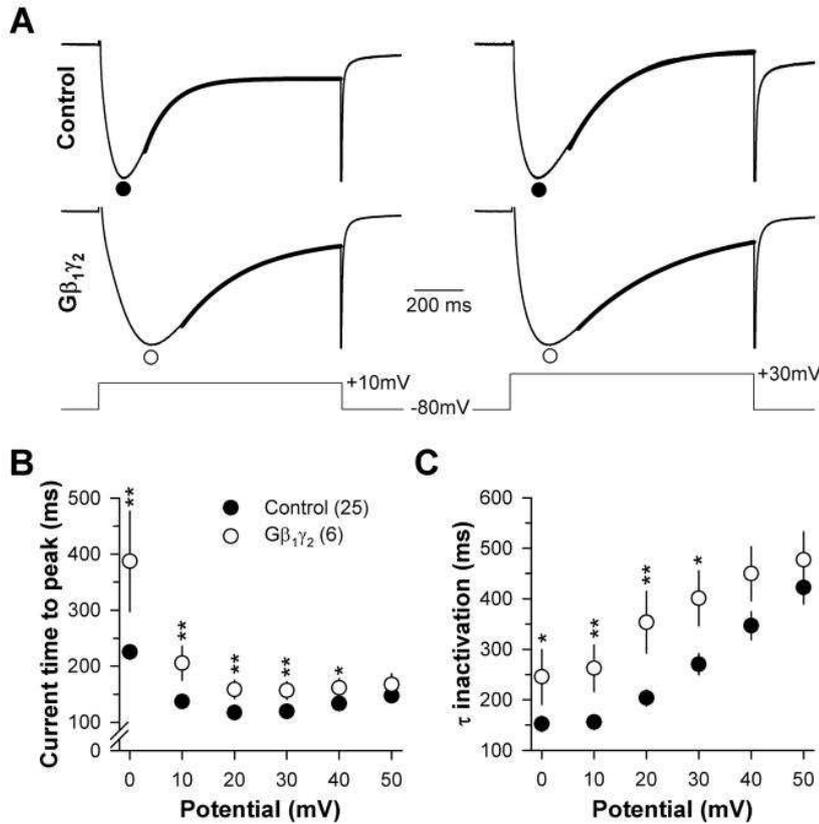
Fig. 5

A strong depolarizing pre-pulse allows recovery from the slowing of L-type calcium current activation induced by $G\beta_1\gamma_2$. **(A)** Representative Ca^{2+} current traces recorded from a control (left panel) and from a $G\beta_1\gamma_2$ dimer-expressing fibre (right panel) in response to a 1 sec long depolarizing step to +20 mV from a holding potential of −80 mV, before (P1) and after (P2) a strong depolarizing pre-pulse (PP) to +100 mV. **(B)** Normalized values (± S.E.M) of P2/P1 peak Ca^{2+} current amplitude as a function of pre-pulse (PP) duration. **(C)** Mean ± S.E.M. values for the time-to-peak of the Ca^{2+} current recorded in P2 as a function of pre-pulse duration. The y axis presents a break point for display purposes. **(D)** Corresponding values for the shift of the Ca^{2+} current time-to-peak between control and $G\beta_1\gamma_2$-expressing fibres as a function of pre-pulse duration. The y axis presents a break point for display purposes.
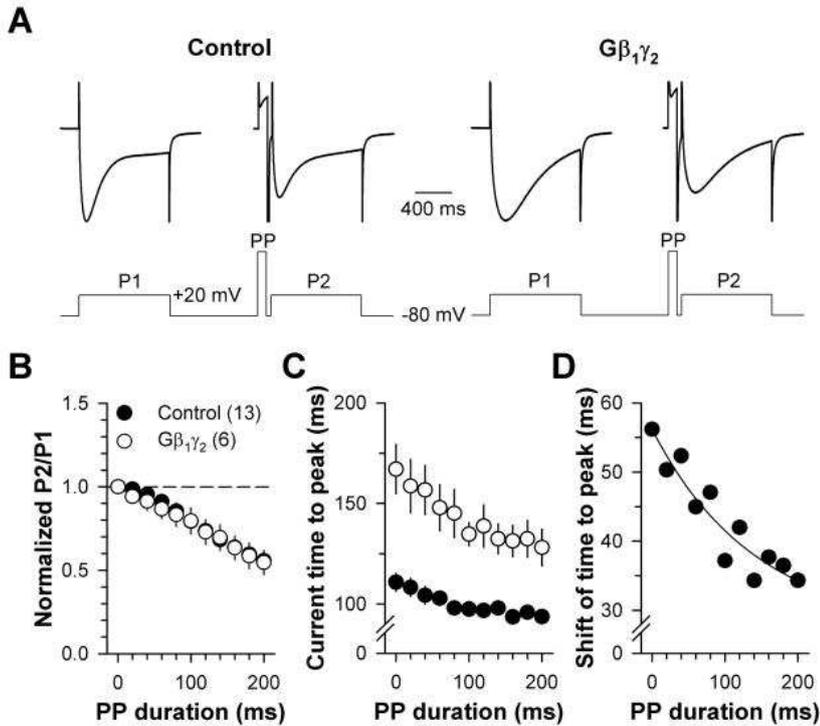
Fig. 6

Expression of G-protein $\beta_1 \gamma_2$ dimers strongly alters the voltage-activated Ca^{2+} transient in skeletal muscle fibres. **(A)** Representative indo-1 saturation traces recorded from a control (left panel) and from a $G\beta_1 \gamma_2$ dimer-expressing fibre (right panel) in response to depolarizing steps of increasing duration to +10 mV from a holding potential of −80 mV. The inset in each panel shows the corresponding mean (continuous traces) ± S.E.M. (grey shading) indo-1 traces. **(B)** Corresponding $[Ca^{2+}]$ traces calculated from the indo-1 signals shown in **(A)**. **(C–D)** Corresponding mean ± S.E.M. values of initial resting $[Ca^{2+}]$ level, peak change in $[Ca^{2+}]$, time constant (τ) of $[Ca^{2+}]$ decay after the end of the pulse and final $[Ca^{2+}]$ level respectively, measured from ten control fibres and six $G\beta_1 \gamma_2$ dimer-expressing fibres. The peak change in $[Ca^{2+}]$ was reduced by 43% (p =0.0003) (20 ms depolarizing step) in the $G\beta_1 \gamma_2$ -expressing fibres.